Czech Technical University in Prague
Faculty of Electrical Engineering

BACHELOR THESIS

Rotary and linear pendulum control

Prague, 2009 **Author: Milan Korda**

Prohlášení

Prohlašuji, že jsem svou bakalářskou práci vypracoval samostatně a použil jsem pouze podklady (literaturu, projekty, SW atd.) uvedené v přiloženém seznamu.

V Praze dne 4.6.2009

podpis

Acknowledgment

Foremost I would like to thank Ing. Petr Hušek, Ph.D. for his excellent leadership. I would also like to thank Ing. Jiří Roubal, Ph.D. for providing valuable technical support to the thesis. Last but not least, I would like to express my gratitude to my family for their support and calm environment they always provided.

Abstract

This thesis deals with identification and control of the cart and pendulum system and the rotary pendulum system. Simultaneous approach is applied to system analysis as well as controller synthesis. Great similarity of both the systems is pointed out during the derivation of the equations of motion using the Euler-Lagrange equation. Several pendulum swing-up techniques are described and compared. The best performance provides sinusoidal-input swing-up and energy-based swing-up strategies, each of which being best suitable for a different purpose. The problem of the pendulum interception at the upright position after the swing-up is also briefly tackled. An LQ controller with integral control and a state estimator is designed and compared to a double loop dynamic output controller designed via root locus techniques. The performance of the LQ controller is far superior to that of the dynamic controller, yet all the basic experiments, including pendulum interception after the swing-up and reference tracking, are successfully carried out with the dynamic controller as well.

Abstrakt

Tato práce se zabývá identifikací a řízením systémů kyvadla na vozíku a rotačního kyvadla. Analýza systémů stejně tak jako návrh řízení jsou provedeny pro oba systémy současně. Velká míra podobnosti obou systému je ukázána během odvození pohybových rovnic pomocí Euler-Lagrangeovy rovnice. Několik způsobů výšvihu kyvadla je popsáno a porovnáno. Nejlepší výsledky vykazují metody výšvihu pomocí sinusového signálu a výšvih založený na měření energie, přičemž každá z těchto metod je nejvhodnější pro jiný účel. Problém zachycení kyvadla po výšvihu v horní poloze je taktéž v krátkosti konfrontován. LQ regulátor s integrálním řízením a pozorovatelem stavu je navržen a porovnán s dvousmyčkovým dynamickým výstupním regulátorem navržrným pomocí metody geometrického místa kořenů. Přestože LQ regulátor podává mnohem lepší výsledký než dynamický regulátor, všechny základní experimenty včetně zachycení kyvadla po výšvihu a sledování referenčního signálu jsou úspěšně provedeny i s dynamickým výstupním regulátorem.

Contents

List of Figures

Chapter 1

Introduction

The cart and pendulum system, which will hereafter be referred to as the linear pendulum, and its slight modification, the rotary pendulum, are classic control theory examples with many practical applications. For instance a Segway vehicle or a space shuttle taking off can be, to some extent, modeled as an inverted pendulum system. On the other hand, a crane moving a cargo is a typical application of such a system with the pendulum hanging downwards. This thesis, however, deals only with the inverted (upright) position.

Both the models are described and identified in chapter 2, where a great similarity of the mathematical models is shown. Therefore, the control of the models will be confronted simultaneously in the next chapters. The Euler-Lagrange equation is used for deriving the equations of motion. A variety of experiments is used for identification of the systems, some of which are, however, not presented in detail in order to keep the work reasonably concise.

Several nonlinear control algorithms for swinging-up the pendulum from the downward to the upright position are outlined in the third chapter. Most of the algorithms are derived from energy-based swing-up proposed in [3]. The algorithms are then compared according to various criteria. A viable swing-up algorithm has to not only ensure that the pendulum reaches the upright position but should also ensure a smooth transition to linear control. Two basic methods to do so are discussed.

The fourth chapter deals with upright position control of the systems. Standard approach to the control of a system with positions and velocities being the only state variables is via state space design methods, which are indeed emphasized in this thesis. Nevertheless, classic dynamic output control is also approached. An LQR (linear quadratic regulator) controller and a double loop dynamic controller are designed and compared not only from a bare performance point of view but also according to synthesis

time consumption and convenience. Strong stabilization of the systems is also briefly discussed. Besides basic experiments such as swing-up and step response, which are performed with both the systems, additional experiments such as sinus tracking or repeated swing-up are performed with the rotary pendulum system only.

Chapter 2

Description and identification

This chapter deals with description and identification of both the linear and the rotary pendulum systems. Firstly, the systems are briefly described, then the equations of motion are derived, and finally the system identification is approached.

2.1 Description of the systems

The linear pendulum system (figure 2.1) consists of a cart and a pendulum that is loosely fastened in the middle of the cart, allowing its free rotation (see figure 2.2). The cart moving on a rail is driven by a DC motor. The input of the system u is motor voltage normalized in the interval $[-1, 1]$. The cart position x [m] measured relatively to the starting point and the pendulum angle φ [rad] measured counterclockwise from the downward position are the outputs of the system.

The rotary pendulum system (figure 2.3) consists of a rotary arm driven by a DC motor and a pendulum loosely fastened at the end of the arm (figure 2.4). The input of the system u is motor voltage normalized in the interval $[-1, 1]$. The output of the model is the angle of the arm θ and the angle of the pendulum φ. Both the angles are measured incrementally and then converted to radians in such a way that the angle orientation is consistent with figure 2.3. The conversion constant is $k_\theta = 8.5719 \cdot 10^{-4}$ rad for the arm angle and $k_\varphi = -3.1403 \cdot 10^{-3}$ rad for the pendulum angle.

The input and output signals are sampled at a period of 0.001 s and 0.005 s for the linear and the rotary pendulum respectively. The systems will be considered continuous throughout the whole thesis.

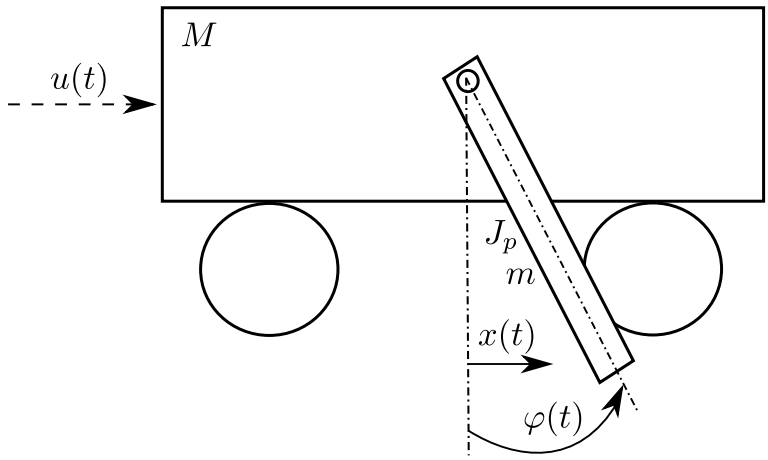

Figure 2.1: *Linear pendulum system*

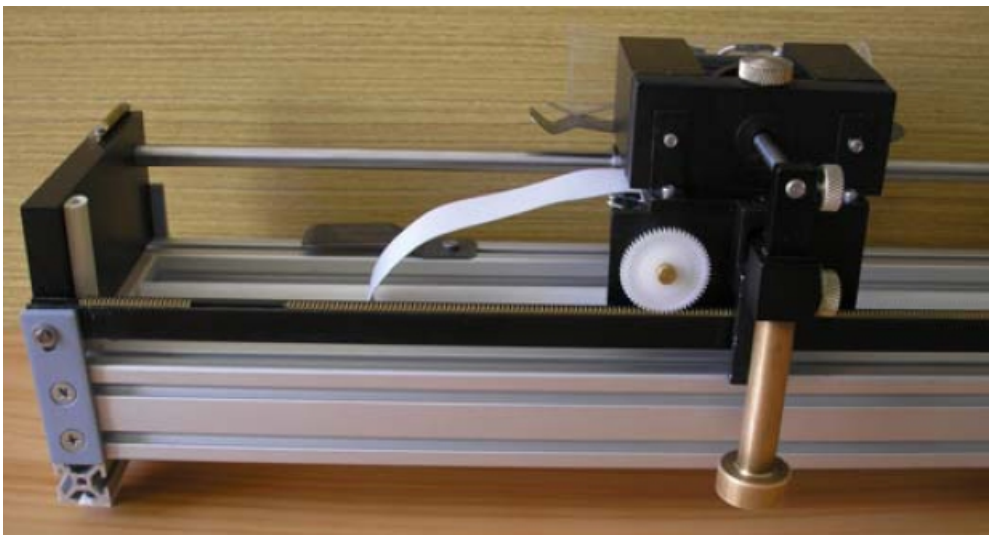

Figure 2.2: *Linear pendulum photograph*

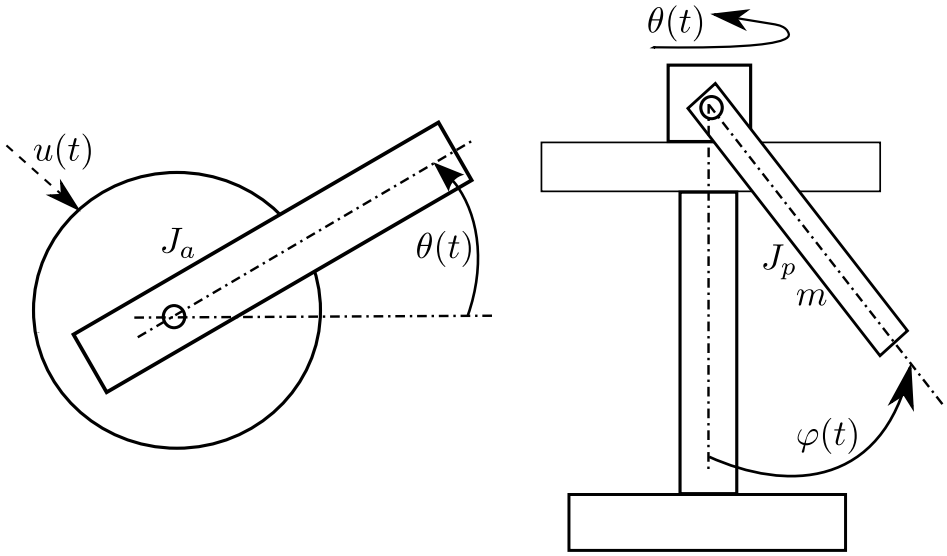

Figure 2.3: *Rotary pendulum system*

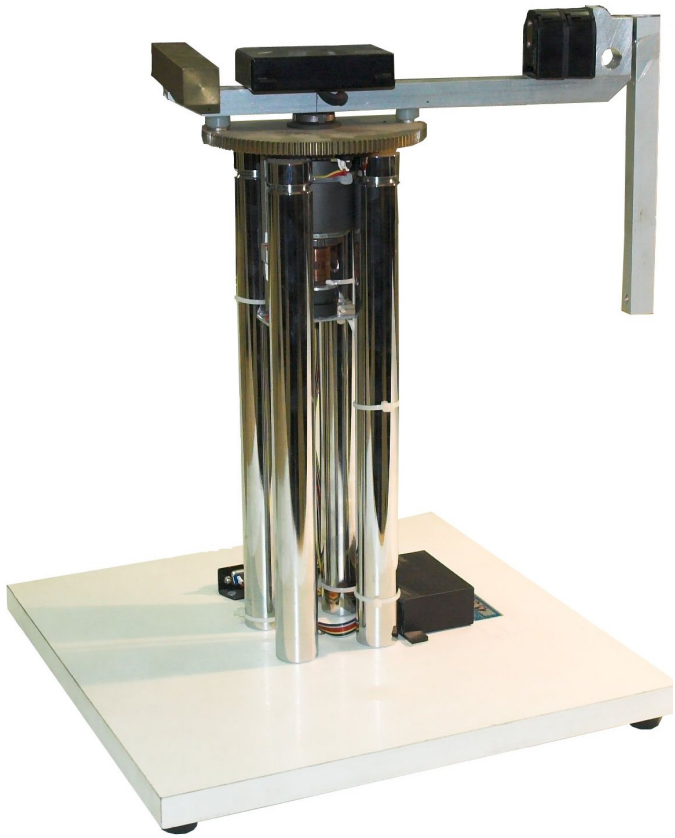

Figure 2.4: *Rotary pendulum photograph*

2.2 Equations of motion

Straight derivation of the equations of motion via Newton's laws would be rather tricky, so the Euler-Lagrange equation [5] is used in order to derive the equations. The Euler-Lagrange equation, which can be derived from the principle of least action, has the form

$$\frac{\mathrm{d}}{\mathrm{d}t}\left(\frac{\partial \mathcal{L}}{\partial \dot{\boldsymbol{q}}}\right) = \frac{\partial \mathcal{L}}{\partial \boldsymbol{q}}, \tag{2.1}$$

where

- $\mathcal{L} = T - U$ is the Lagrangian of the system, T is the kinetic energy of the system and U is the potential energy of the system,
- $\boldsymbol{q}$ is the vector of generalized coordinates.

In this form, equation (2.1) can be used for frictionless systems only. Thus, the equations of motion are firstly derived under zero friction assumption, and the friction is added at the end of the process.

Once the kinetic and potential energy of the system are determined, the derivation is straightforward but still lengthy, so only the Lagrangian of both the systems is derived here. For the kinetic energy of a rigid body holds

$$T = \frac{1}{2}\int_m \boldsymbol{v}^2 \,\mathrm{d}m. \tag{2.2}$$

The velocity $\boldsymbol{v}$ of each element of the pendulum rod is the sum $\boldsymbol{V} + \boldsymbol{v_i}$, where $\boldsymbol{V}$ is the pivot point velocity, and $\boldsymbol{v_i} = \boldsymbol{\omega} \times \boldsymbol{r_i}$ is the velocity of the element with respect to the pivot. Then, the kinetic energy of the pendulum is

$$T_p = \frac{1}{2}\int_m (\boldsymbol{V} + \boldsymbol{v_i})^2 \,\mathrm{d}m = \frac{1}{2} mV^2 + \boldsymbol{V} \cdot \left(\boldsymbol{\omega} \times \int_m \boldsymbol{r_i} \,\mathrm{d}m\right) + \frac{1}{2} J_p \omega^2, \tag{2.3}$$

where

- m [kg] is the mass of the pendulum,
- J_p [kg m^2] is the moment of inertia of the pendulum with respect to the pivot,
- $\boldsymbol{\omega}$ [rad/s] is the angular velocity of the pendulum.

The second term on the right-hand side of equation (2.3) is equal to

$$m\boldsymbol{V} \cdot (\boldsymbol{\omega} \times \boldsymbol{r_{\mathrm{cm}}}) = mlV\omega\cos\varphi,$$

where

- $\boldsymbol{r}_{\mathbf{cm}}$ [m] is the position vector of the center of mass of the pendulum rod,
- l [m] is the length of the projection of $\boldsymbol{r}_{\mathbf{cm}}$ on the axis perpendicular to the axis of rotation and the instantaneous velocity (with respect to the pivot) of the center of mass.

The potential energy of the system is

$$U = -mgl\cos\varphi + U_0, \tag{2.4}$$

where

- U_0 [J] is an arbitrary constant, which doesn't affect the equations of motion. The constant was chosen as $U_0 = -mgl$, so that the upright position potential energy is equal to zero.
- g [ms^{-2}] is gravitational acceleration.

Considering the fact that the $\boldsymbol{V} = \dot{x}$ for the linear pendulum and $\boldsymbol{V} = R\dot{\theta}$ (where R is the distance between the pivot points of the arm and of the pendulum) for the rotary pendulum, the Lagrangian is

$$\mathcal{L} = \frac{1}{2}(M+m)\dot{x}^2 + ml\dot{x}\omega\cos\varphi + \frac{1}{2}J_p\dot{\varphi}^2 + mgl\cos\varphi - U_0, \tag{2.5}$$

for the linear pendulum, and

$$\mathcal{L} = \frac{1}{2}(J_a + mR^2)\dot{\theta}^2 + mlR\dot{\theta}\omega\cos\varphi + \frac{1}{2}J_p\dot{\varphi}^2 + mgl\cos\varphi - U_0, \tag{2.6}$$

for the rotary pendulum.

Now it's obvious that both the systems will be described by differential equations of the exact same form. Setting $\boldsymbol{q} = [x\ \varphi]$ for the linear and $\boldsymbol{q} = [\theta\ \varphi]$ for the rotary pendulum, and applying equation (2.1) yields

$$(M+m)\ddot{x} + ml\ddot{\varphi}\cos\varphi - ml\dot{\varphi}^2\sin\varphi = 0 \tag{2.7}$$

$$J_p\ddot{\varphi} + mgl\sin\varphi + ml\ddot{x}\cos\varphi = 0, \tag{2.8}$$

for the linear pendulum, and

$$(J_a + mR^2)\ddot{\theta} + ml\ddot{\varphi}\cos\varphi - ml\dot{\varphi}^2\sin\varphi = 0 \tag{2.9}$$

$$J_p\ddot{\varphi} + mgl\sin\varphi + mlR\ddot{\theta}\cos\varphi = 0, \tag{2.10}$$

for the rotary pendulum.

After introducing friction terms, model input and after slight rearrangement with substitution of some constants, the equations become

$$\ddot{x} + b\dot{x} + \mu \operatorname{sgn} \dot{x} = Ku - K_1\ddot{\varphi}\cos\varphi + K_1\dot{\varphi}^2\sin\varphi \tag{2.11}$$

$$\ddot{\varphi} + 2\delta\dot{\varphi} + \mu_p \operatorname{sgn} \dot{\varphi} + \omega_n^2 \sin\varphi = -K_2\ddot{x}\cos\varphi, \tag{2.12}$$

for the linear pendulum, and

$$\ddot{\theta} + b\dot{\theta} + \mu \operatorname{sgn} \dot{\theta} = Ku - K_1\ddot{\varphi}\cos\varphi + K_1\dot{\varphi}^2\sin\varphi \tag{2.13}$$

$$\ddot{\varphi} + 2\delta\dot{\varphi} + \mu_p \operatorname{sgn} \dot{\varphi} + \omega_n^2 \sin\varphi = -K_2\ddot{\theta}\cos\varphi \tag{2.14}$$

for the rotary pendulum, where

- u is the input of the system,
- K is the motor constant,
- b is a viscose friction coefficient of the cart or the arm which also represents motor dynamics,
- δ is a viscose friction damping coefficient of the pendulum,
- μ, μ_p are Coulomb friction coefficients,
- ω_n is the natural frequency of the pendulum,
- K_1, K_2 are constants that represent interaction between the pendulum and the cart (or the arm).

2.3 Identification

All the coefficients in equations 2.11 – 2.14 had to be identified. Good overall performance of the nonlinear model was the goal of the linear pendulum system identification, whereas only the upright position accuracy of the model was considered with the rotary pendulum. Being more important for the control of the system, pendulum angle accuracy was emphasized in both cases. In general terms, identification process was quite similar in both cases.

First of all, coefficients describing pendulum dynamics ω_n, δ and μ_p were determined. Initial condition response to displaced pendulum for the maximum angle such that the cart (or arm) doesn't move is suitable for this purpose. If the angle was too small, the Coulomb friction term would be dominant, hence preventing proper evaluation of the viscose friction term. A linear approximation of the pendulum equation is a good starting point for determination of the natural frequency and the viscose friction terms.

The cart/arm and motor dynamics constants b, μ and the motor constant K were identified from step response of the system.

The interaction constants K_1 and K_2 were determined from overall system response to various input steps and initial conditions with emphasis on upright position accuracy in the rotary pendulum case. Some of the already identified constants were also slightly modified in order to achieve good overall performance of the models.

Because of unmodeled nonlinearities, precise identification is, of course, nearly impossible (and was not a goal).

Numerical values of identified parameters for the linear pendulum are:

$$\begin{aligned} K &= 5.98\,\mathrm{m/s^2} & K_2 &= 15.57\,\mathrm{rad/m} \\ K_1 &= 0.00537\,\mathrm{m/rad} & \omega_n &= 10.84\,\mathrm{rad/s} \\ b &= 3.42\,\mathrm{s^{-1}} & \delta &= 0.098\,\mathrm{s^{-1}} \\ \mu &= 0.245\,\mathrm{m/s^2} & \mu_p &= 0.184\,\mathrm{rad/s^2} \end{aligned}$$

The parameters of the rotary pendulum system are

$$\begin{aligned} K &= 108.6\,\mathrm{rad/s^2} & K_2 &= 1.7485\,\mathrm{rad/m} \\ K_1 &= 0.0335 & \omega_n &= 8.83\,\mathrm{rad/s} \\ b &= 3.41\,\mathrm{s^{-1}} & \delta &= 0.198\,\mathrm{s^{-1}} \\ \mu &= 0.246\,\mathrm{rad/s^2} & \mu_p &= 0.2\,\mathrm{rad/s^2} \end{aligned}$$

2.4 Linearization

Both the systems are described by fourth order nonlinear model. The state vector of the system was chosen as $\boldsymbol{x} = [\dot{x}\ x\ \dot{\varphi}\ \varphi]^{\mathrm{T}}$ for the linear pendulum and $\boldsymbol{x} = [\dot{\theta}\ \theta\ \dot{\varphi}\ \varphi]^{\mathrm{T}}$ for the rotary pendulum. Assuming zero input, there are two sets of equilibrium points: the downward position equilibrium set

$$\boldsymbol{x_0} = [0\ \ x_0|\theta_0\ \ 0\ \ 2k\pi]^{\mathrm{T}},$$

and the upright position equilibrium set

$$\boldsymbol{x_0} = [0 \;\; x_0 | \theta_0 \;\; 0 \;\; (2k+1)\pi]^{\mathrm{T}},$$

where k is an integer number, and x_0 or θ_0 is an arbitrary position of the cart or the arm. This result is, of course, completely intuitive.

As the sgn function cannot be linearized, the Coulomb friction terms were omitted during the linearization, and the model coefficients were slightly adjusted to preserve reasonable accuracy.

Final form of the equations suitable for linearization is

$$\ddot{x} + 3.93\dot{x} = 5.98u - 0.006\ddot{\varphi}\cos(\varphi) + 0.006\dot{\varphi}^2\sin(\varphi) \tag{2.15}$$

$$\ddot{\varphi} + 0.54\dot{\varphi} + 117.51\sin(\varphi) = -14.13\ddot{x}\cos(\varphi) \tag{2.16}$$

for the linear pendulum, and

$$\ddot{\theta} + 3.419\dot{\theta} = 108.55u - 0.0134\ddot{\varphi}\cos(\varphi) + 0.0134\dot{\varphi}^2\sin(\varphi) \tag{2.17}$$

$$\ddot{\varphi} + 0.44\dot{\varphi} + 75.69\sin(\varphi) = -1.929\ddot{x}\cos(\varphi) \tag{2.18}$$

for the rotary pendulum.

The standard linearization method via Jacobian matrix has been used.

2.4.1 Linearized model of the linear pendulum

Despite the fact that the system is to be controlled at the upright position only, the model was also linearized at the downward position in order to compare its accuracy with the nonlinear model and the real system.

The linear state space model at the upright position is

$$\dot{\boldsymbol{x}} = \boldsymbol{A}\boldsymbol{x} + \boldsymbol{B}u = \begin{bmatrix} -4.298 & 0 & 0.00357 & 0.7758 \\ 1 & 0 & 0 & 0 \\ -60.76 & 0 & -0.5904 & 128.47 \\ 0 & 0 & 1 & 0 \end{bmatrix} \boldsymbol{x} + \begin{bmatrix} 6.541 \\ 0 \\ 92.45 \\ 0 \end{bmatrix} u \tag{2.19}$$

$$\boldsymbol{y} = \boldsymbol{C}\boldsymbol{x} + \boldsymbol{D}u = \begin{bmatrix} 0 & 0 & 0 & 1 \\ 0 & 1 & 0 & 0 \end{bmatrix} \boldsymbol{x} + \begin{bmatrix} 0 \\ 0 \end{bmatrix} u, \tag{2.20}$$

where $\boldsymbol{y} = [\varphi \;\; x]^{\mathrm{T}}$ is the output vector.

The transfer functions at the upright position are

$$P_\varphi(s) = \frac{\varphi(s)}{u(s)} = \frac{92.45s}{s^3 + 4.889s^2 - 126.1s - 505.1}, \tag{2.21}$$

$$P_x(s) = \frac{x(s)}{u(s)} = \frac{6.541s^2 + 3.532s - 768.6}{s^4 + 4.889s^3 - 126.1s^2 - 505.1s}. \tag{2.22}$$

The poles of the system are

$$\text{poles} = \{-11.918;\ -3.884;\ 0;\ 10.913\} \tag{2.23}$$

The zeros of P_φ are

$$\text{zeros}_\varphi = \{0\},$$

and the zeros of P_x are

$$\text{zeros}_x = \{-11.113;\ 10.573\}.$$

Therefore, the system is, as expected, unstable, and the cart transfer function is nonminimum phase.

Since downward position control is not discussed in this thesis, only the downward position state space model is presented here. The model is

$$\dot{\boldsymbol{x}} = \begin{bmatrix} -4.298 & 0 & 0.00357 & 0.7758 \\ 1 & 0 & 0 & 0 \\ 60.76 & 0 & -0.5904 & -128.47 \\ 0 & 0 & 1 & 0 \end{bmatrix} \boldsymbol{x} + \begin{bmatrix} 6.541 \\ 0 \\ -92.45 \\ 0 \end{bmatrix} u$$

$$\boldsymbol{y} = \begin{bmatrix} 0 & 0 & 0 & 1 \\ 0 & 1 & 0 & 0 \end{bmatrix} \boldsymbol{x} + \begin{bmatrix} 0 \\ 0 \end{bmatrix} u.$$

2.4.2 Linearized model of the rotary pendulum

As mentioned before, only upright position accuracy was considered during the rotary pendulum identification, and the model was, therefore, linearized at the upright position only.

The linear state space model at the upright position is

$$\dot{\boldsymbol{x}} = \boldsymbol{A}\boldsymbol{x} + \boldsymbol{B}u = \begin{bmatrix} -3.595 & 0 & -0.01497 & 2.765 \\ 1 & 0 & 0 & 0 \\ -6.257 & 0 & -0.4461 & 82.429 \\ 0 & 0 & 1.0 & 0 \end{bmatrix} \boldsymbol{x} + \begin{bmatrix} 115.28 \\ 0 \\ 200.66 \\ 0 \end{bmatrix} u \tag{2.24}$$

$$\boldsymbol{y} = \boldsymbol{C}\boldsymbol{x} + \boldsymbol{D}u = \begin{bmatrix} 0 & 0 & 0 & 1 \\ 0 & 1 & 0 & 0 \end{bmatrix} \boldsymbol{x} + \begin{bmatrix} 0 \\ 0 \end{bmatrix} u, \tag{2.25}$$

where $\boldsymbol{y} = [\varphi\ \theta]^{\mathrm{T}}$ is the output vector.

The transfer functions at the upright position are

$$P_\varphi(s) = \frac{\varphi(s)}{u(s)} = \frac{200.7s}{s^3 + 4.041s^2 - 80.92s - 279}, \tag{2.26}$$

$$P_\theta(s) = \frac{\theta(s)}{u(s)} = \frac{115.3s^2 + 48.42s - 8947}{s^4 + 4.041s^3 - 80.92s^2 - 279s}. \tag{2.27}$$

The poles of the system are

$$\text{poles} = \{-9.4736;\ -3.3522;\ 0;\ 8.7852\} \tag{2.28}$$

The zeros of P_φ are

$$\text{zeros}_\varphi = \{0\},$$

and the zeros of P_θ are

$$\text{zeros}_\theta = \{-9.0225;\ 8.6025\}.$$

Again, the system is unstable, and the cart transfer function is nonminimum phase.

2.5 Model comparison

In this section, the linear and nonlinear models are compared with the real system. Only a small portion of performed experiments is presented in order to preserve the conciseness of the work. For instance, the frequency responses of the systems, which sinusoidal-input swing-up (3.7) is based on, are omitted.

2.5.1 Linear pendulum model comparison

Step response at the downward position and initial condition response at the upright position[1] were used in order to examine the accuracy of the models.

[1]Using an initial condition equal to $\boldsymbol{x_0} = [0\ 0\ 0\ \pi]$ wouldn't have led to any movement; therefore a number slightly smaller then π was used instead.

As intended, accuracy of the pendulum angle is, especially at the upright position, rather good. Slightly worse accuracy of the cart position is, then, not an issue for the control.

The step response is depicted in figures 2.5, 2.6, 2.7. The initial condition response is then depicted in figure 2.8.

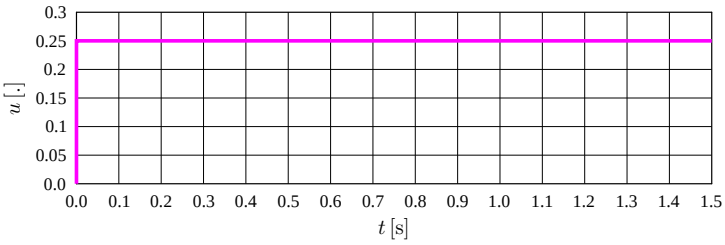

Figure 2.5: *Downward position step response – input*

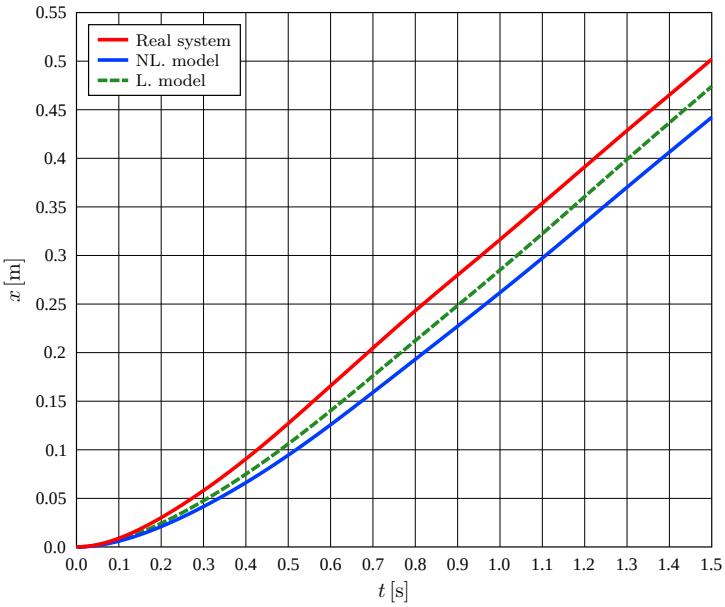

Figure 2.6: *Downward position step response – cart position*

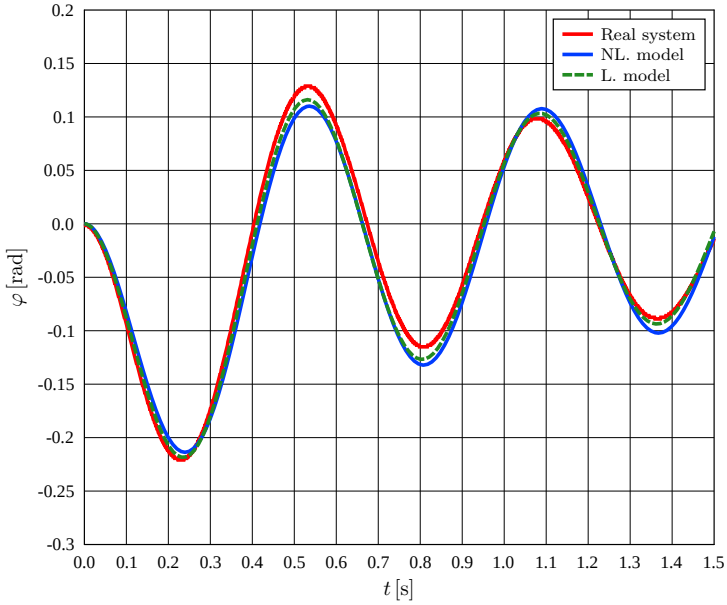

Figure 2.7: *Downward position step response – pendulum angle*

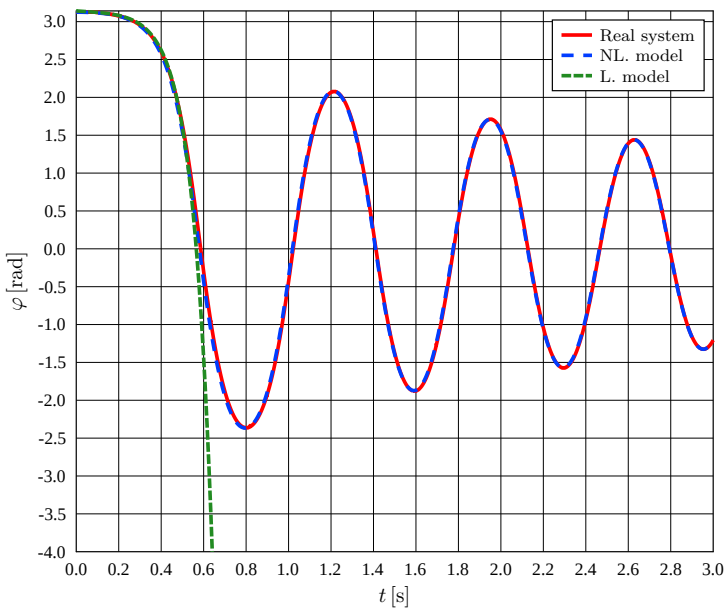

Figure 2.8: *Upright position initial condition response – pendulum angle*

2.5.2 Rotary pendulum model comparison

Upright position accuracy being the primary concern, mainly the results of upright position experiments are presented here. Upright position step response and, again, upright position initial condition response were examined. The only presented downward position experiment is the step response of the arm.

Since it's necessary to hold the pendulum rod in fingers until a step is initiated, there is large uncertainty at the beginning of the upright position step response, producing poor reproducibility of such an experiment. Nevertheless, the results of the experiment are still presented.

Accuracy of the model is slightly worse then the one of the linear pendulum, but still sufficient enough for effective feedback control.

The upright position step response is depicted in figures 2.9, 2.10 and 2.11, the initial condition response then in figure 2.12. Figures 2.13 and 2.14 show the downward position step response.

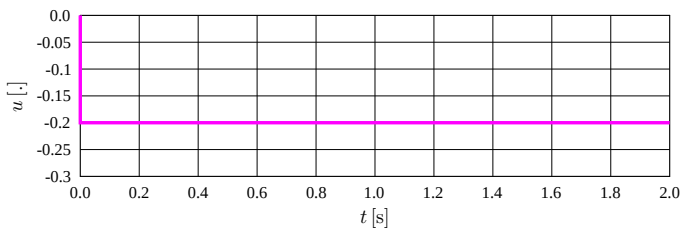

Figure 2.9: *Upright position step response – input*

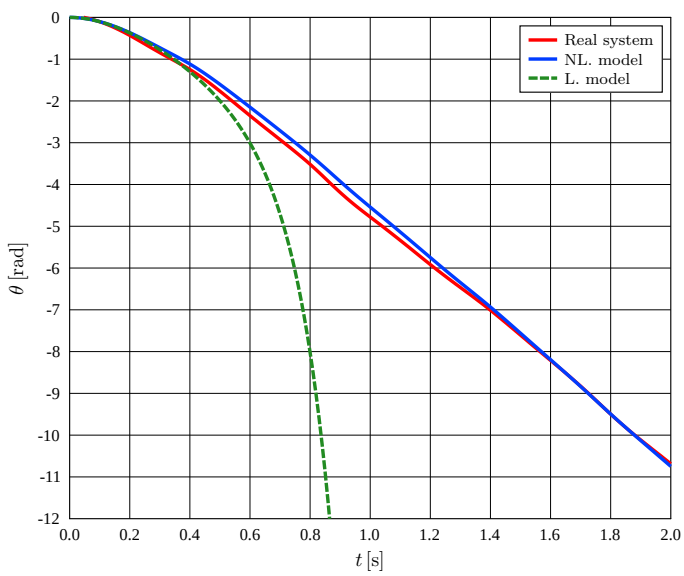

Figure 2.10: *Upright position step response – arm position*

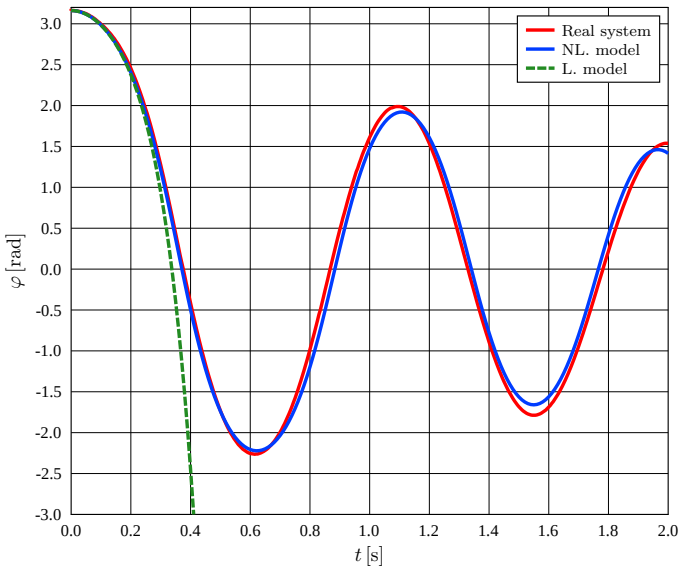

Figure 2.11: *Upright position step response – pendulum angle*

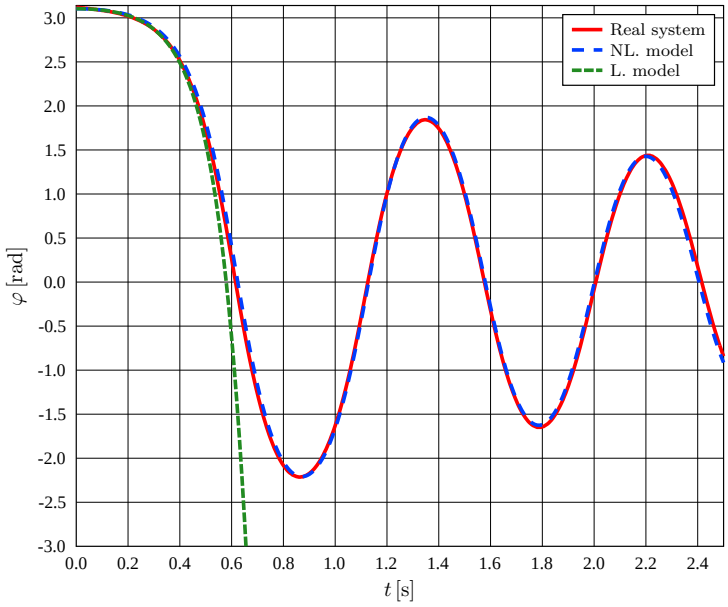

Figure 2.12: *Upright position initial condition response – pendulum angle*

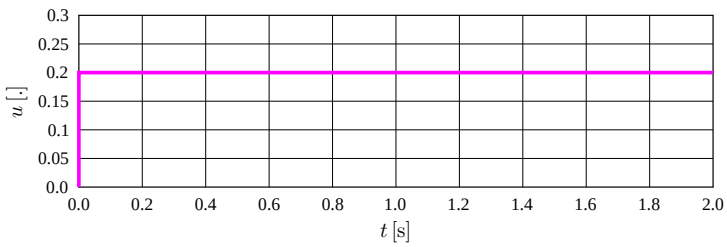

Figure 2.13: *Downward position step response – input*

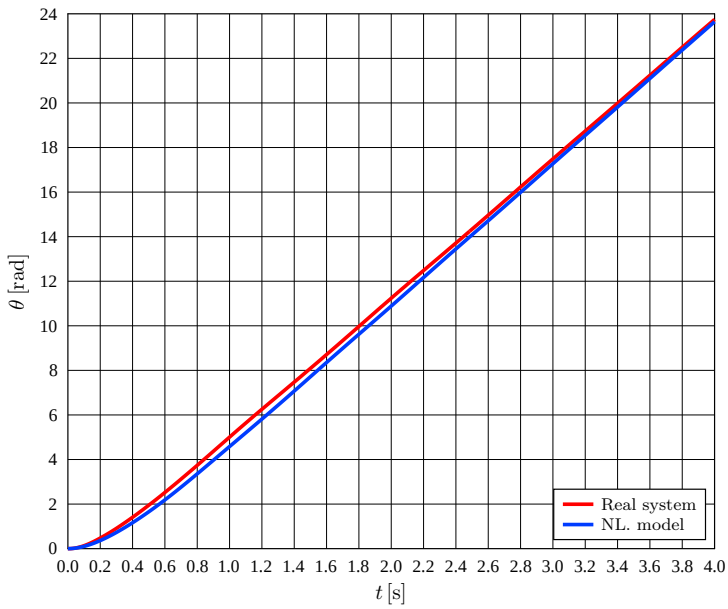

Figure 2.14: *Downward position step response – arm position*

Chapter 3

Pendulum swing-up

One feedforward and several feedback algorithms for pendulum swing-up are outlined in this chapter. All the feedback algorithms are based on energy considerations.

Once the pendulum reaches the upright position it's necessary to catch and stabilize it there. Only basic techniques, which are nonetheless completely sufficient for its purpose, are discussed in this chapter.

3.1 Feedback algorithms

3.1.1 Theoretical analysis

Equation (2.8) was examined in order to derive an energy based control law [3]. Analysis of the swing-up is, of course, completely analogous for the rotary pendulum.

The total energy of a pendulum is

$$E = T + U = \frac{1}{2} J_p \dot{\varphi}^2 - mgl \cos\varphi - mgl. \tag{3.1}$$

Taking first time derivative of the total energy and substituting from equation (2.8) yields

$$\dot{E} = J_P \ddot{\varphi}\dot{\varphi} + mgl\dot{\varphi}\sin\varphi = -ml\ddot{x}\dot{\varphi}\cos\varphi \tag{3.2}$$

which immediately implies a simple control law maximizing energy pumped into the system:

$$u = -u_{\max}\,\mathrm{sgn}(\dot{\varphi}\cos\varphi) = \begin{cases} u_{\max}, & \dot{\varphi}\cos\varphi < 0 \\ -u_{\max}, & \dot{\varphi}\cos\varphi > 0. \end{cases} \tag{3.3}$$

Such a control law would, however, lead to unacceptably large cart displacement, and thus smaller magnitude of the input signal had to be taken. Choice of the magnitude is dependent on a particular system and will be briefly discussed later.

Another issue to tackle is the speed of the pendulum rod when approaching the upright position. Considering bounded system input, large value of the speed would make it impossible for the controller to catch the pendulum rod at the upright position. A speed constraint can be, however, easily formulated in the terms of energy based control. The control action is simply set to zero as the energy of the pendulum reaches the value corresponding to the upright position potential energy. This leads to a modified control law[1]

$$u = -u_{\max} \operatorname{sgn}\left((E - E_0)\dot{\varphi}\cos\varphi\right), \tag{3.4}$$

where E_0 is the potential energy at the upright position (which has been set to zero) or any other energy value to be reached.

Swing-up from any initial condition is, then, theoretically possible with such a control law. The control law is, therefore, suitable especially for repeated swing-up after the pendulum falls from the upright position as will be shown with the rotary pendulum system.

3.1.2 Real system application analysis

Since the real system is not frictionless, control law (3.4) with energy overshoot ($E_0 > 0$) was used. Hysteresis was also introduced in order to avoid oscillations around zero. This control law was, however, used only with the rotary pendulum where repeated swing-up experiments were carried out.

With proper choice of $u_{\max}$, simpler version 3.3, not involving energy computation, can be used for swing-up from the downward position zero speed initial condition, which is the most common case.

Simplified energy-based control law 3.3 was compared with two more or less intuitively conjectured control laws. The laws are zero speed switching

$$u = -u_{\max} \operatorname{sgn}\dot{\varphi} = \begin{cases} u_{\max}, & \dot{\varphi} < 0 \\ -u_{\max}, & \dot{\varphi} > 0 \end{cases} \tag{3.5}$$

[1] Assuming $\operatorname{sgn}(0) = 0$.

and zero angle switching

$$u = -u_{\max} \operatorname{sgn} \varphi = \begin{cases} u_{\max}, & \varphi < 0 \\ -u_{\max}, & \varphi > 0. \end{cases} \tag{3.6}$$

The zero speed switching turns out to be a simplification of the energy based swing-up.

Proper choice of the input signal magnitude $u_{\max}$ is crucial to catch the pendulum at the upright position and to keep cart (or arm) displacement small. Reasonable values of the magnitude that ensures successful swing-up are

$$\begin{aligned} u_{\max} &= 0.5 \text{ for } \dot{\varphi} \cos \varphi = 0 \text{ switching (3.3)}, \\ u_{\max} &= 0.6 \text{ for } \dot{\varphi} = 0 \text{ switching (3.5)}, \\ u_{\max} &= 0.7 \text{ for } \varphi = 0 \text{ switching (3.6)}, \end{aligned}$$

in the linear pendulum case and

$$\begin{aligned} u_{\max} &= 0.16 \text{ for } \dot{\varphi} \cos \varphi = 0 \text{ switching (3.3)}, \\ u_{\max} &= 0.26 \text{ for } \dot{\varphi} = 0 \text{ switching (3.5)}, \\ u_{\max} &= 0.20 \text{ for } \varphi = 0 \text{ switching (3.6)}, \\ u_{\max} &= 0.26 \text{ for energy-based swing-up (3.4)}, \end{aligned}$$

in the rotary pendulum case.

3.2 Feedforward swing-up

Feedforward swing-up using sinusoidal input at resonance frequency of the system proves to be the most effective way of swing-up from the downward position zero speed initial condition. A major drawback of this method is the impossibility of swing-up from a large subset of the system phase space, making it ultimately suitable for swing-up from the downward position equilibrium only.

The input signal with this swing-up method has the form

$$u(t) = A \sin(\omega t + \psi), \tag{3.7}$$

where ω is chosen around the resonance frequency of the transfer function $\varphi(s)/u(s)$ at the downward position. When chosen to be 0 or π, the phase shift ψ affects only the direction of the first approach to the upright position. The signal amplitude A has to be

tuned such that the pendulum speed is modest nearby the upright position. The signal was chosen as

$$u(t) = 0.85 \sin(11t + \pi) \tag{3.8}$$

for the linear pendulum and

$$u(t) = 0.29 \sin(9.6t) \tag{3.9}$$

for the rotary pendulum.

3.3 Pendulum interception

The pendulum rod has to be caught and stabilized when approaching the upright position. The simplest way to do so, so-called hard switch, is to switch to the linear control when the pendulum is close enough to the upright position. Linear region $|\varphi - \pi| < \pi/6$ works fine for both the systems.

Slightly more sophisticated way proposed in [4], so-called soft switch, consists in introducing an intermediate region where the control action is obtained as a weighted sum of linear controller and swing-up control actions. An intermediate region from $\pi/6$ to $\pi/12$ of the distance from π provides good performance. Control action within this region is given by

$$u = (1 - \alpha)u_{\text{swing}} + \alpha u_{\text{cont}} \ ; \quad \alpha = 2 - \frac{12}{\pi} |\varphi - \pi|. \tag{3.10}$$

3.4 Real system application

All the above described swing-up techniques were compared on the real systems. Even though the hard switch interception of the pendulum would have been satisfactory for both the systems, the soft switch was used instead in the rotary pendulum case, slightly improving transition between swing-up and linear control[1].

[1] Linear control with cart/arm position reference tracking is provided by an LQ controller described in section 4.1.

3.4.1 Linear pendulum swing-up responses

Responses for the linear system are in figures 3.1, 3.2, 3.3. As mentioned above, the best performance in the terms of least swing-up time provides the sinusoidal input control followed by the zero speed switching and the zero $\dot{\varphi}\cos\varphi$ switching. The longest swing-up time provides the zero angle switching, which is in accordance with the energy considerations discussed in paragraph 3.1.1.

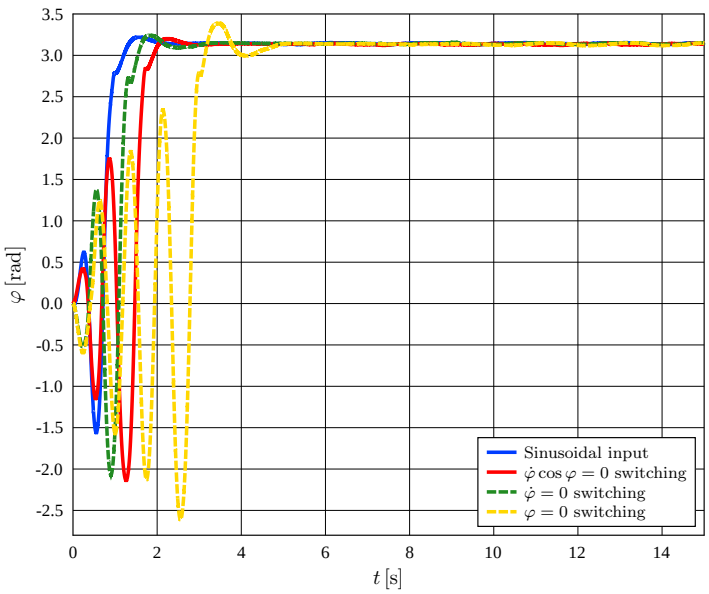

Figure 3.1: *Linear pendulum swing-up – pendulum angle*

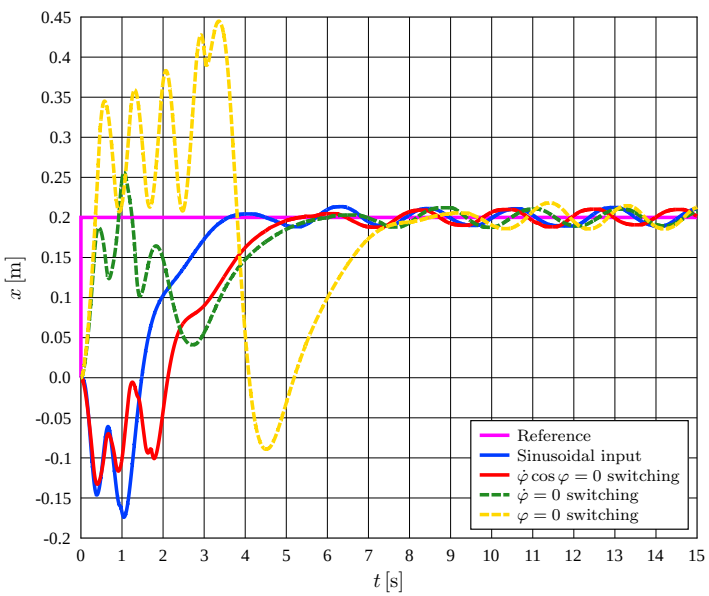

Figure 3.2: *Linear pendulum swing-up – cart position*

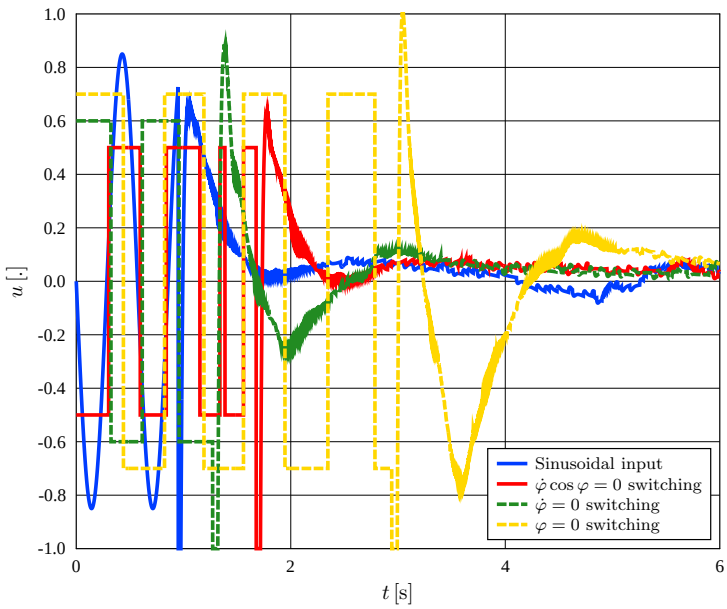

Figure 3.3: *Linear pendulum swing-up – control action*

3.4.2 Rotary pendulum swing-up responses

Responses for the linear system are in figures 3.4, 3.5, 3.6. The best performance again provides the sinusoidal input control this time, however, followed by the zero $\dot{\varphi}\cos\varphi$ switching and the zero angle switching. The worst performance of the zero speed switching is due to fairly long time intervals where the angle of the pendulum is larger then $\pi/2$ and therefore the energy is being removed from the pendulum during those intervals.

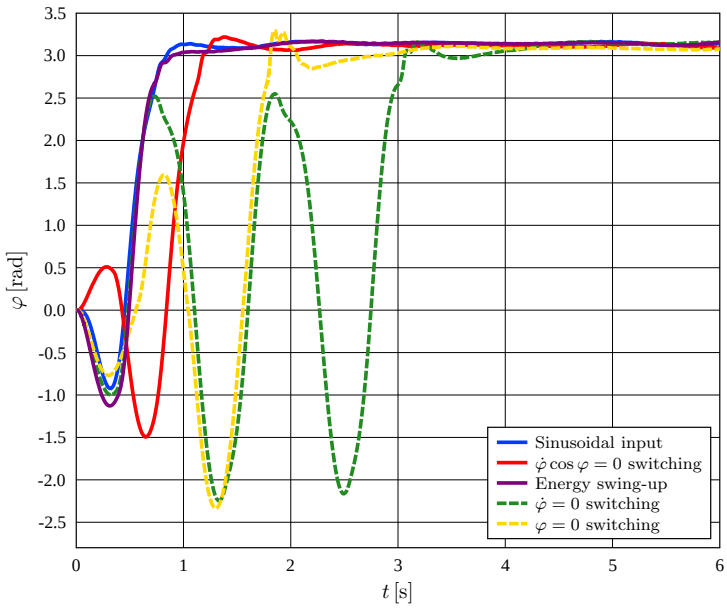

Figure 3.4: *Rotary pendulum swing-up – pendulum angle*

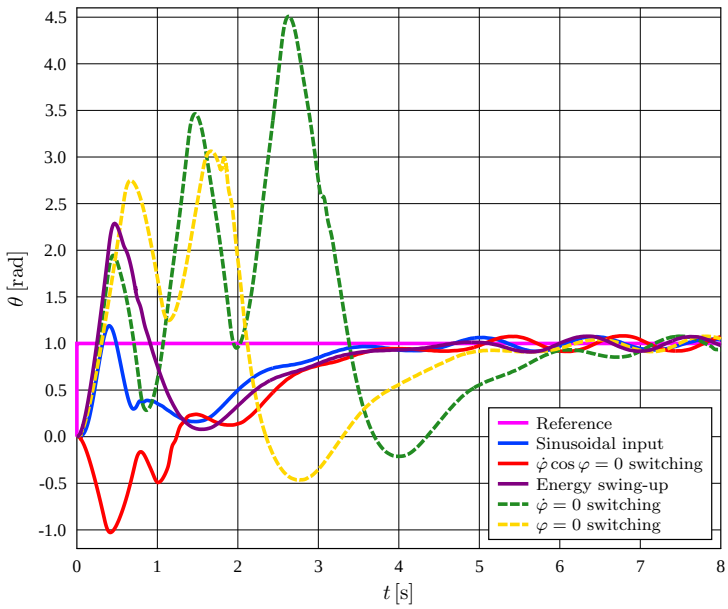

Figure 3.5: *Rotary pendulum swing-up – arm angle*

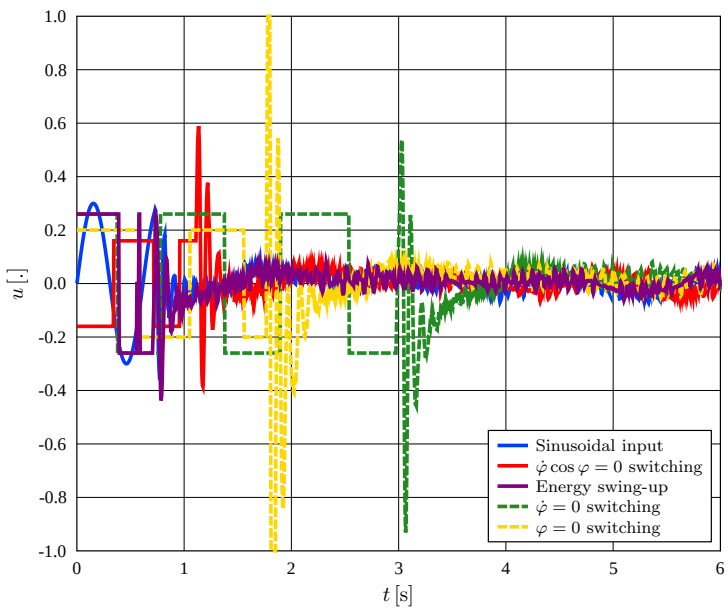

Figure 3.6: *Rotary pendulum swing-up – control action*

Chapter 4

Control of the systems

Proper upright position control design is crucial for successful pendulum interception as well as for robust stabilization of the pendulum rod and cart/arm position reference tracking. State space design methods were emphasized, even though dynamic output controllers were also designed for both the systems. All the controllers were designed in such a way that a reasonable compromise between the magnitude of oscillations around equilibrium points and robustness properties was reached. Design patterns are similar for both the systems and thus are treated simultaneously whenever possible.

4.1 State space control

Design of an LQ controller with a state estimator and integral control to eliminate steady state error of the cart/arm position is described in this section. A diagram of the state space control with swing-up is depicted in figure 4.1

4.1.1 State feedback design

Controllability matrices of both the systems extended with an integrator have a full rank, and thus the systems are controllable (and hence stabilizable). Linear quadratic optimal state feedback was obtained as the control law $u = -\boldsymbol{K}\hat{\boldsymbol{x}}$ that minimizes the quadratic cost function

$$J(u) = \int_0^\infty (\hat{\boldsymbol{x}}^{\mathrm{T}}\boldsymbol{Q}\hat{\boldsymbol{x}} + u^{\mathrm{T}}\boldsymbol{R}u),$$

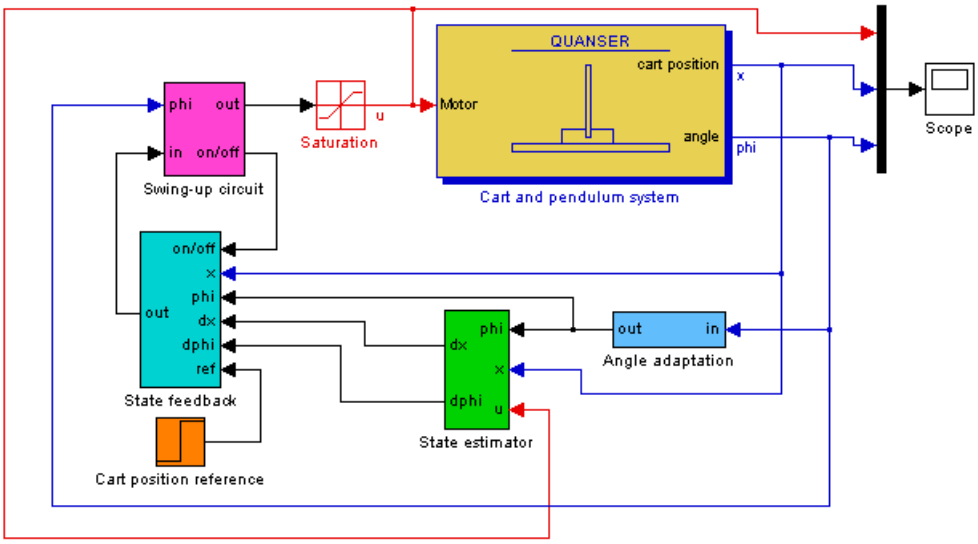

Figure 4.1: *State space control with swing-up*

where $\hat{\boldsymbol{x}} = [\boldsymbol{x}^{\mathrm{T}} \ x_{\mathrm{I}}]^{\mathrm{T}}$ denotes the extended state vector with state x_{I} representing the integral of the cart position error. $\boldsymbol{Q}$, $\boldsymbol{R}$ are weighting matrices such that $\boldsymbol{Q}$ is positive semidefinite, $\boldsymbol{R}$ is positive definite and the pair $(\boldsymbol{A},\ \boldsymbol{Q}^{1/2})$ is detectable. This choice of the weighting matrices along with the stabilizability of the system ensures that the solution to the LQ optimization problem exists, can be obtained as a full-state feedback, and that the feedback system is asymptotically stable[1]. After a short trial-and-error process, the weighting matrices were chosen as $\boldsymbol{Q} = \mathrm{diag}(1\ 6\ 1\ 4\ 20)$, $\boldsymbol{R} = 6$ for the linear pendulum and $\boldsymbol{Q} = \mathrm{diag}(1\ 10\ 1\ 30\ 20)$, $R = 4$ for the rotary pendulum, which results in an LQ optimal state feedback

$$\boldsymbol{K} = \begin{bmatrix} -2.5024 & -2.7817 & 0.6670 & 6.0394 & 1.8257 \end{bmatrix}$$

for the linear pendulum and

$$\boldsymbol{K} = \begin{bmatrix} -1.2852 & -2.8475 & 1.3755 & 11.890 & 2.2361 \end{bmatrix}$$

for the rotary pendulum. The poles of the feedback system are

$$\{-1.2717 \pm 0.9392i,\ -3.2567 \pm 1.7455i,\ -41.1264\}$$

for the linear pendulum and

$$\{-1.6445,\ -2.9568,\ -5.5440 \pm 2.1616i,\ -116.2009\}$$

[1]Certain robustness in terms of the phase and gain margins is also ensured for single input systems [1].

for the rotary pendulum.

These settings were used for all the experiments presented in section 4.3. However, a more conservative control law with lower weights on the arm position and the arm position error integral is better suited for repeated swing-up experiments because of fairly large arm displacement that might occur during such experiments. Satisfactory results with the rotary pendulum provides, for instance, the choice of the weighting matrices $\boldsymbol{Q} = \mathrm{diag}(1\ 0.01\ 1\ 60\ 0.6)$, $\boldsymbol{R} = 4$. Repeated swing-up experiments were not performed with the linear pendulum.

The arm displacement not being limited, tracking of an arbitrarily large input step should be ensured by the controller. This is, however, not the case due to the inherent nonlinear nature of the system (e.g. input saturation). This difficulty can be resolved by limiting the rate of change of the reference signal. An acceptable value of the limitation negligible for small steps is 14 rad/s.

A diagram of the state feedback with the integral control is in figure 4.2. The switch in the diagram only turns off the integration of the cart/arm position error during the swing-up process.

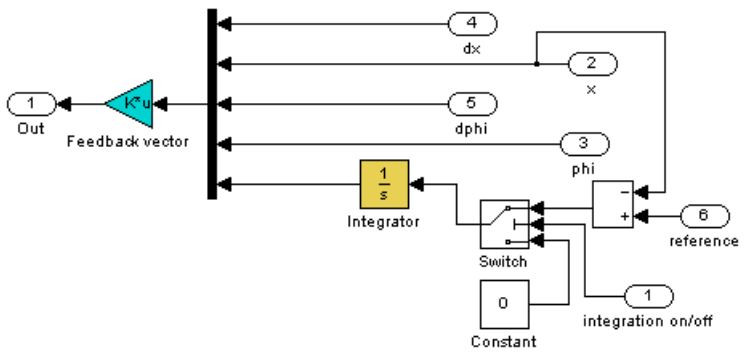

Figure 4.2: *State feedback with integral control*

4.1.2 Estimator design

The observability matrices of both the systems have a full rank. The states of the systems are therefore observable through the cart/arm position and the angle of the pendulum. Since the velocity of the cart/arm and the angle velocity of the pendulum are not measured, a full-order state estimator was designed. However, only the states that are not measured are fed back from the estimator, whereas the remaining states are fed back directly from the plant. It's easy to see that the separation principle still holds. Because

the system is not very much affected by noise, the poles of the estimator were chosen relatively fast at

$$\{-42,\ -39,\ -36,\ -24\}$$

for the linear pendulum and at

$$\{-60,\ -56,\ -32,\ -24\}$$

for the rotary pendulum, which yields the sate-injection matrix

$$\boldsymbol{L} = \begin{bmatrix} 496.08 & 53.276 & -2414.2 & -40.228 \\ -184.53 & -5.4217 & 2131.6 & 82.835 \end{bmatrix}^{\mathrm{T}}$$

for the linear pendulum and

$$\boldsymbol{L} = \begin{bmatrix} 1187.8 & 80.354 & -704.48 & -11.018 \\ -176.32 & -3.9801 & 1842.9 & 87.606 \end{bmatrix}^{\mathrm{T}}$$

for the rotary pendulum.

An estimator designed using the Kalman-Bucy filtering theory [1] was tried out for both the systems. The optimality in the original sense of the optimal filtering problem was, however, not intended to achieve, and such thing is, in fact, nearly impossible because of unknown probabilistic properties of the noise. Therefore, the Kalman-Bucy filter design was only used as an alternative tuning method of the state estimator. The quantization error of the output sensors served as the first estimate of the measurement noise covariance. The process noise covariance matrix coefficients were used purely as tuning parameters.

The process noise covariance matrix $\boldsymbol{Q}$ and the measurement noise covariance matrix $\boldsymbol{R}$ providing a decent performance are $\boldsymbol{Q} = \mathrm{diag}(1\ 0.001\ 1\ 0.001)$, $\boldsymbol{R} = \mathrm{diag}(10^{-7}\ 10^{-7})$ for the linear pendulum and $\boldsymbol{Q} = \mathrm{diag}(8\ 0.004\ 8\ 0.004)$, $\boldsymbol{R} = \mathrm{diag}(10^{-6}\ 10^{-6})$ for the rotary pendulum, which yields the state injection matrix

$$\boldsymbol{L} = \begin{bmatrix} 2393.3 & 120.94 & -3794.3 & -40.06 \\ -394.46 & -4.006 & 2189.9 & 72.245 \end{bmatrix}^{\mathrm{T}}$$

for the linear pendulum and

$$\boldsymbol{L} = \begin{bmatrix} 2490.1 & 94.72 & -358.91 & -2.823 \\ -187.95 & -2.82 & 2903.8 & 98.99 \end{bmatrix}^{\mathrm{T}}$$

for the rotary pendulum. The estimator poles with these matrices are

$$\{-94.14,\ -48.51,\ -27.71 \pm 27.16i\}$$

for the linear pendulum and

$$\{-47.88 \pm 21.61i,\ -51.00 \pm 18.36i\}$$

for the rotary pendulum.

The model of the estimator is a standard full-order estimator model, and hence is not presented here.

4.2 Dynamic controller

Double loop dynamic controllers were designed via root locus techniques for both the systems. A diagram of the double loop control is in figure 4.3.

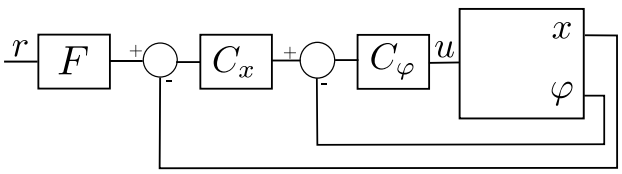

Figure 4.3: *Double loop dynamic control*

The inner loop controls the pendulum angle, while the outer loop controls cart/arm position. Feedforward filter only improves step response performance. Both the outer loop and inner loop controllers were designed using Matlab *sisotool*. The inner one, C_φ, with the transfer function P_φ, the outer one then with the transfer function $P_x C_\varphi/(1+P_\varphi C_\varphi)$, where all common factors had been canceled. Filter F was designed to cancel stable closed loop zeros, reducing the step response overshoot.

It's worth noting that the inner loop controllers are, not by a coincidence, unstable. In fact, according to [8] the P_φ transfer functions are not strongly stabilizable since there is an odd number (actually one) of poles in between right half plane zeros, which are at 0 and ∞. Therefore, no stable controller exists for P_φ.

The transfer functions are

$$C_\varphi(s) = \frac{6.302s^2 + 94.68s + 263.2}{s^2 + 19.11s - 9.661}, \quad C_x(s) = \frac{-4.4s - 13.33}{s + 33.33},$$

$$F(s) = \frac{1}{\left(\frac{s}{11.341}+1\right)\left(\frac{s}{11.113}+1\right)\left(\frac{s}{3.683}+1\right)\left(\frac{s}{3.030}+1\right)}$$

for the linear pendulum and

$$C_\varphi(s) = \frac{9.866s^2 + 130.2s + 321.3}{s^2 + 50.62s - 23.34}, \quad C_x(s) = \frac{-0.3857s - 0.4285}{s + 5.556},$$

$$F(s) = \frac{1}{\left(\frac{s}{9.947}+1\right)\left(\frac{s}{8.977}+1\right)\left(\frac{s}{3.286}+1\right)\left(\frac{s}{1.109}+1\right)}$$

for the rotary pendulum.

4.3 Simulation results

Pendulum interception followed with a step response served as a basic experiment to examine the performance of the controllers for both the systems. Several interesting experiments such as sinus reference tracking or repeated swing-up after the pendulum falls due to a large disturbance were also carried out for the rotary pendulum.

The LQ controller outperforms the dynamic one in virtually any criterion: the oscillation amplitudes of both the cart/arm position and the pendulum angle are lower, cart/arm displacement during pendulum interception is smaller and robustness in terms of disturbance rejection is better. Unlike with the dynamic controller, the mean value of the cart/arm position error is zero with the LQ controller. Nevertheless, the dynamic controller still provides decent performance as both swing-up and reference tracking are possible.

4.3.1 Linear pendulum

Swing-up and the step response simulations results for the linear pendulum system are in figures 4.4, 4.5, 4.6. Some interesting experiments successfully carried out such as swing-up and control on a gentle slope of the cart rail are not presented here.

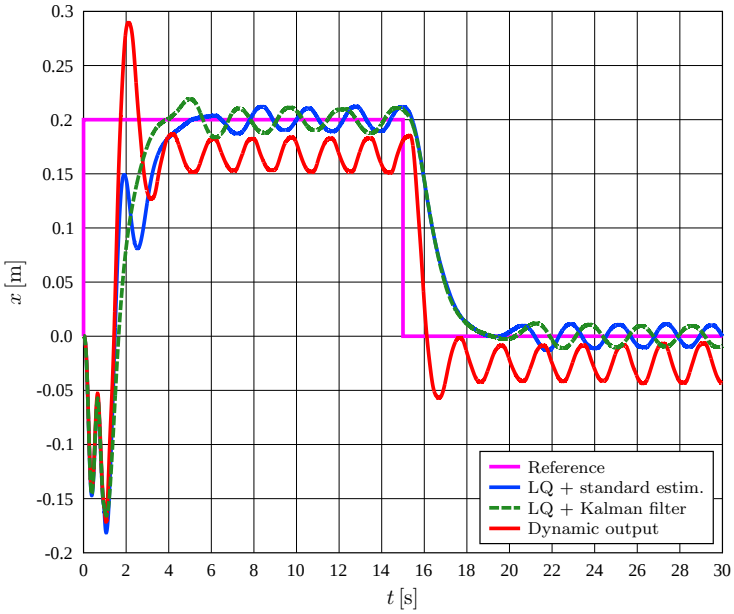

Figure 4.4: *Linear pendulum: swing-up and step response – cart position*

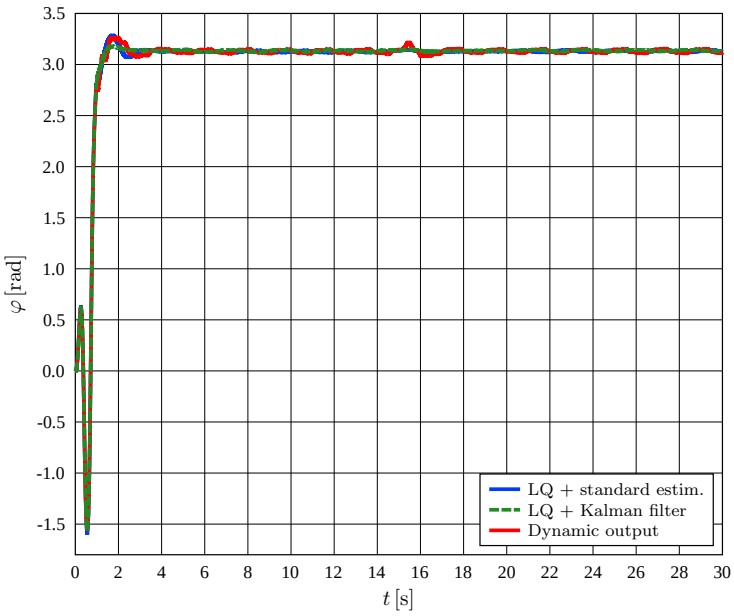

Figure 4.5: *Linear pendulum: swing-up and step response – pendulum angle*

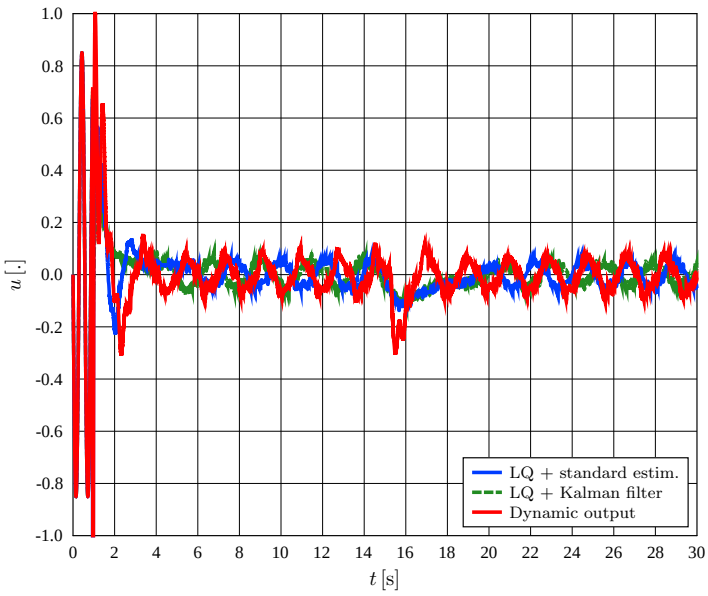

Figure 4.6: *Linear pendulum: swing-up and step response – control action*

4.3.2 Rotary pendulum

Swing-up and the step response simulations results for the rotary pendulum system are in figures 4.7, 4.8, 4.9. Sinus reference tracking responses with the LQ controller are then in figures 4.10, 4.11, 4.12. The pendulum angle during the repeated swing-up experiment is depicted in figure 4.13.

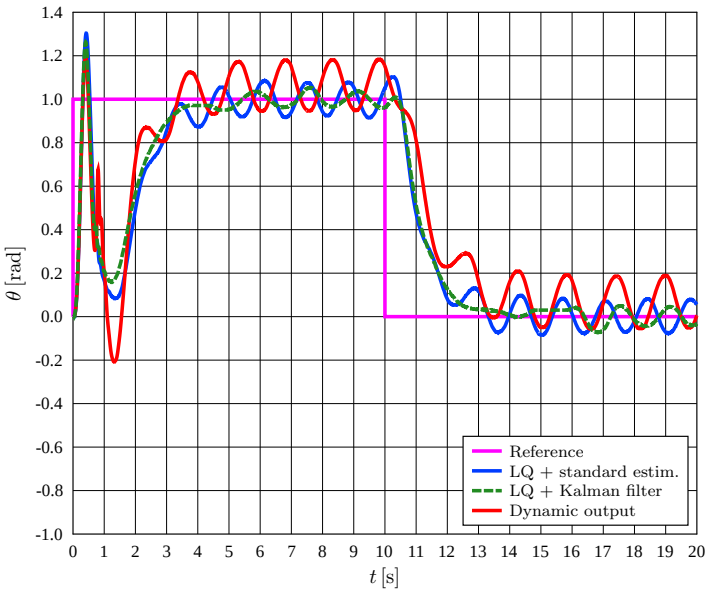

Figure 4.7: *Rotary pendulum: swing-up and step response – cart position*

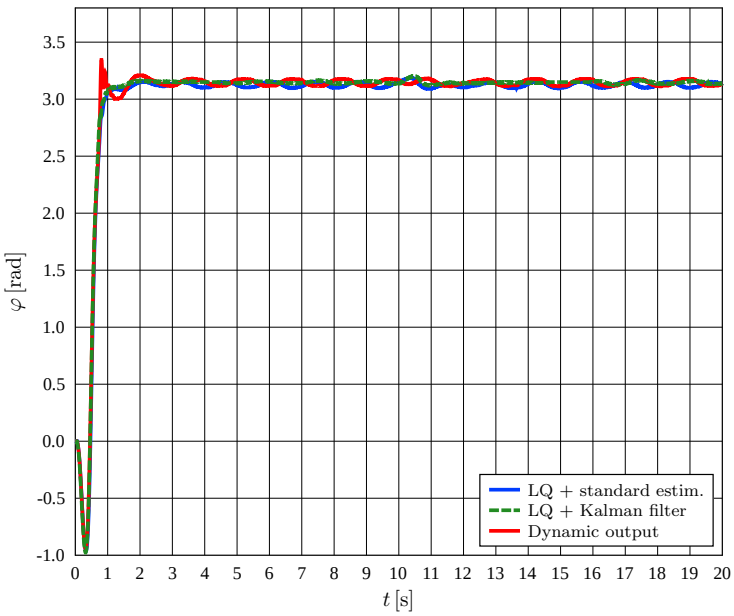

Figure 4.8: *Rotary pendulum: swing-up and step response – pendulum angle*

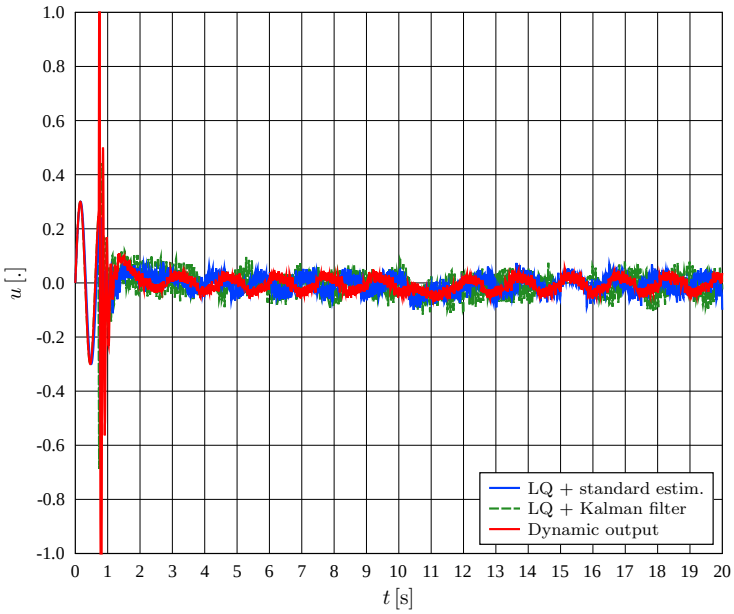

Figure 4.9: *Rotary pendulum: swing-up and step response – control action*

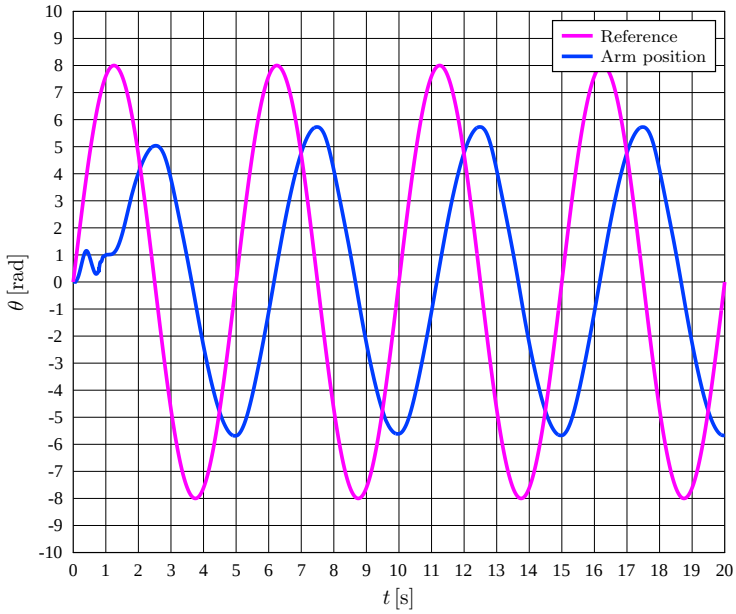

Figure 4.10: *Rotary pendulum: sinus reference tracking – cart position*

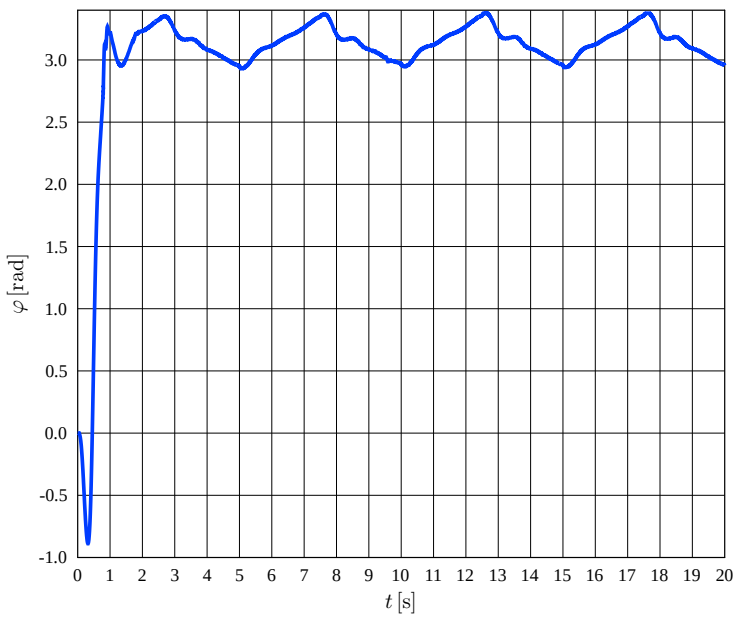

Figure 4.11: *Rotary pendulum: sinus reference tracking – pendulum angle*

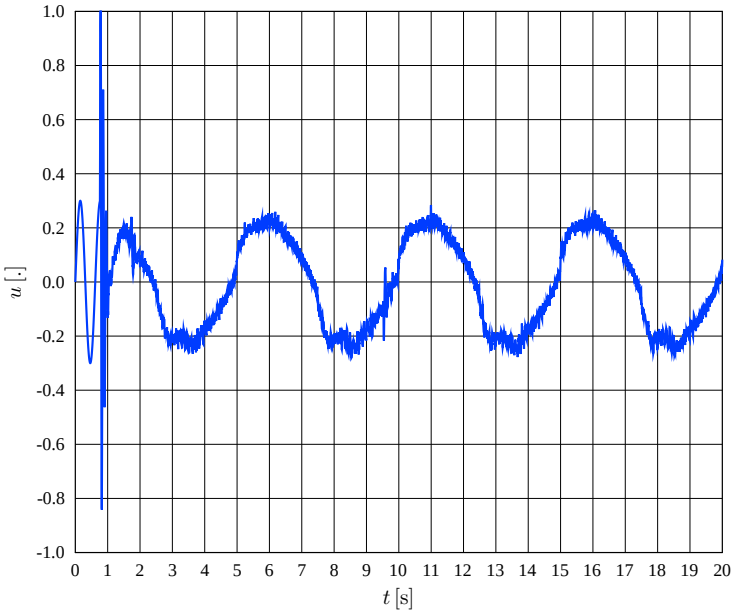

Figure 4.12: *Rotary pendulum: sinus reference tracking – control action*

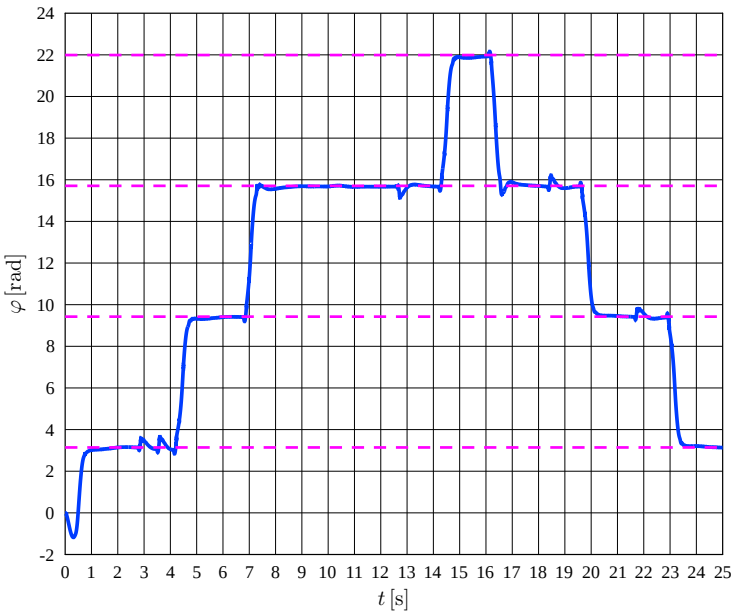

Figure 4.13: *Rotary pendulum: repeated swing-up – pendulum angle*

Chapter 5

Conclusion

It has been shown that both the rotary and linear pendulum systems are described with, from a control theory point of view, an identical set of nonlinear differential equations. The coefficients of the equations were identified using various experiments, emphasizing overall accuracy of the model for the linear pendulum and upright position accuracy for the rotary pendulum. The nonlinear equations were then linearized at the upright position equilibrium. Achieved accuracy of the models is completely sufficient for controller design purposes.

Several swing-up methods were outlined and compared. For swing-up from the downward position equilibrium, the best performance is provided by the sinusoidal-input-at-resonance-frequency swing-up method, which is, however, not suitable for swing-up from other points of the system phase space. On the other hand, energy-based swing-up method proposed in [3] overcomes this drawback, theoretically enabling swing-up from any point of the phase space. Moreover, this method performs only slightly worse during swing-up from the downward position equilibrium than the sinusoidal input method does. Apart from hard switching between the swing-up and linear control algorithms, soft switching with a transition region between the two algorithms was introduced for the rotary pendulum, slightly improving transition smoothness.

Dynamic output root locus and state space LQ design methods were set against each other. The LQ controller surpasses the dynamic output one in terms of the control performance as well as in terms of synthesis tediousness. LQ design via tuning weighting matrices of an LQ criterion and state estimator pole placement is far more time-efficient than rather tedious and not so intuitive design of a double loop dynamic controller. Nevertheless, design of a dynamic controller that performs similarly to the LQ controller is not beyond the scope of the root locus method. In fact, an LQ controller with state

estimator is, of course, an output dynamic controller with a different structure designed via a completely different technique.

A Simulink demo of the swing-up and control process has been created as a motivation for undergraduate as well as graduate courses in control theory. The nonlinear model of the rotary pendulum has also been used in a Matlab Virtual Reality model for educational purposes. Finally, there has been a contribution to the rotary pendulum system description on website [9].

Bibliography

[1] Anderson, Brian D.O. and Moore, John B. *Optimal Control Linear Quadratic Methods*. Dover Publications, Mineola, 2007.

[2] Antsaklis, Panos J. and Michel, Anthony N. *A Linear Systems Primer*. Birkhäuser, Boston, 2007.

[3] Åström, Karl J. and Furuta, Katsuhisa. *Swinging up a pendulum by energy control*. Automatica, 2000.

[4] Bugeja, Marvin. *Non-Linear Swing-Up and Stabilizing Control of an Inverted Pendulum System*. EUROCON 2003, Ljubljana, 2003.

[5] Feynman, Richard P., Leighton, Robert B., and Sands, Matthew. *The Feynman Lectures on Physics: The Definitive and Extended Edition*. Addison-Wesley, 2005.

[6] Franklin, Gene F., Powell, J. David, and Emami-Naeini, Abbas. *Feedback control of dynamic systems*. Pearson Prentice Hall, New Jersey, 5th edition, 2006.

[7] Furuta, Katsuhisa and Iwase, Masami. *Swing-up time analysis of pendulum*. Bulletin of The Polish Academy of Sciences, 2004.

[8] Jia, Yingmin and Ackermann, Jürgen. *Condition and algorithm for simultaneous stabilization of linear plants*. Automatica, 2001.

[9] Roubal, Jiří. Laboratory of Automatic Control Theory [online]. [cit. 2009-01-16], ⟨http://support.dce.felk.cvut.cz/lab26⟩, 2009.

Appendix A

Contents of the attached CD

A CD with Matlab source codes, Simulink models and other materials is attached to the thesis. The contents of the CD is divided into the following directories.

- *Text*: contains the electronic version of the thesis text.
- *Models*: contains the Simulink models and Matlab source codes.
- *Videos*: contains videos of some of the experiments made with the rotary pendulum.